

Ca²⁺-dependent regulation of a non-selective cation channel from *Aplysia* bag cell neurones

Derek A. Lupinsky and Neil S. Magoski

Department of Physiology, Queen's University, Kingston, ON, Canada, K7L 3N6

Ca²⁺-activated, non-selective cation channels feature prominently in the regulation of neuronal excitability, yet the mechanism of their Ca²⁺ activation is poorly defined. In the bag cell neurones of *Aplysia californica*, opening of a voltage-gated, non-selective cation channel initiates a long-lasting afterdischarge that induces egg-laying behaviour. The present study used single-channel recording to investigate Ca²⁺ activation in this cation channel. Perfusion of Ca²⁺ onto the cytoplasmic face of channels in excised, inside-out patches yielded a Ca²⁺ activation EC₅₀ of 10 μM with a Hill coefficient of 0.66. Increasing Ca²⁺ from 100 nM to 10 μM caused an apparent hyperpolarizing shift in the open probability (*P*_o) versus voltage curve. Beyond 10 μM Ca²⁺, additional changes in voltage dependence were not evident. Perfusion of Ba²⁺ onto the cytoplasmic face did not alter *P*_o; moreover, in outside-out recordings, *P*_o was decreased by replacing external Ca²⁺ with Ba²⁺ as a charge carrier, suggesting Ca²⁺ influx through the channel may provide positive feedback. The lack of Ba²⁺ sensitivity implicated calmodulin in Ca²⁺ activation. Consistent with this, the application to the cytoplasmic face of calmodulin antagonists, calmidazolium and calmodulin-binding domain, reduced *P*_o, whereas exogenous calmodulin increased *P*_o. Overall, the data indicated that the cation channel is activated by Ca²⁺ through closely associated calmodulin. Bag cell neurone intracellular Ca²⁺ rises markedly at the onset of the afterdischarge, which would enhance channel opening and promote bursting to elicit reproduction. Cation channels are essential to nervous system function in many organisms, and closely associated calmodulin may represent a widespread mechanism for their Ca²⁺ sensitivity.

(Received 25 January 2006; accepted after revision 6 June 2006; first published online 8 June 2006)

Corresponding author N. S. Magoski: Department of Physiology, Queen's University, 4th Floor, Botterell Hall, 18 Stuart Street, Kingston, ON, Canada, K7L 3N6. Email: magoski@post.queensu.ca

Found in the nervous systems of all species examined, Ca²⁺-activated, non-selective cation channels set excitability and firing rates (Partridge *et al.* 1979; Swandulla & Lux, 1985; Morisset & Nagy, 1999; Egorov *et al.* 2002), tune information processing (Hall & Delaney, 2000; Van den Abbeele *et al.* 1994), and play roles in neuropathology (Fraser & MacVicar, 1996; Chen *et al.* 1997; Smith *et al.* 2003). These channels are non-selective to monovalent cations, may be Ca²⁺ permeable or voltage dependent, and typically show activation at ~1 μM intracellular Ca²⁺, but can respond over the nanomolar to millimolar range (Yellen, 1982; Partridge & Swandulla, 1987, 1988; Razani-Boroujerdi & Partridge, 1993; Cho *et al.* 2003; Liman, 2003; Liu & Liman, 2003; Prawitt *et al.* 2003; Guinamard *et al.* 2004).

Particularly in the nervous system, the means by which Ca²⁺-activated cation channels transduce Ca²⁺ is not fully understood. The ubiquitous Ca²⁺-binding protein, calmodulin, mediates the Ca²⁺-dependent activation,

inactivation, or facilitation of many ion channel species (Saimi & Kung, 2002; Xia *et al.* 1998; Levitan, 1999; Michikawa *et al.* 1999; Zuhlke *et al.* 1999). In addition, the effect of Ca²⁺ on ligand-gated cation channels, such as cyclic nucleotide-gated (CNG) channels (Liu *et al.* 1994; Bradley *et al.* 2004) and NMDA receptors (Krupp *et al.* 1999; Rycroft & Gibb, 2004), is due to closely associated calmodulin. Moreover, calmodulin is the Ca²⁺ sensor for a non-neuronal, transient receptor potential/melastatin (TRPM) cation channel, expressed in heart, pancreas, kidney, and intestine (Launay *et al.* 2002; Nilius *et al.* 2005). However, for native, neuronal, steady-state, Ca²⁺-activated cation channels, the mechanism of Ca²⁺ sensitivity remains unknown.

The present study examines the Ca²⁺-dependent activation and modulation of a non-selective cation channel from the bag cell neurones of the marine snail, *Aplysia californica*. This channel provides the depolarizing drive for the afterdischarge, a prolonged burst that initiates

egg-laying behaviour (Kupfermann, 1967; Kupfermann & Kandel, 1970; Pinsker & Dudek, 1977; Conn & Kaczmarek, 1989). The afterdischarge is characterized by ~ 30 min of action potential firing, with a concomitant release and influx of Ca^{2+} that results in the neurohaemal secretion of egg-laying hormone (Fink *et al.* 1988; Fisher *et al.* 1994). Upon termination of the afterdischarge, a lengthy refractory period ensues, during which a second burst cannot be elicited (Conn & Kaczmarek, 1989). Previously, Wilson *et al.* (1996) found that elevating Ca^{2+} , from nanomolar to micromolar levels, at the cytoplasmic face of patches excised from bag cell neurones increased cation channel activity; however, the extent or the mechanisms of Ca^{2+} activation were not examined. We now provide evidence to suggest that closely associated calmodulin serves as the cation channel Ca^{2+} sensor. Linking the cation channel and calmodulin provides a means to translate a change in intracellular Ca^{2+} into a change in excitability, which, in a system like the bag cell neurones, is essential for triggering behaviour. As a whole, calmodulin may act in this capacity for neuronal cation channels throughout the metazoa.

Methods

Animals and cell culture

Adult *Aplysia californica* weighing 150–300 g were obtained from Marinus Inc. (Long Beach, CA, USA). Animals were housed in an ~ 300 l aquarium containing continuously circulating, aerated sea water (Instant Ocean; Aquarium Systems, Mentor, OH, USA or Kent sea salt; Kent Marine, Acworth, GA, USA) at 14–16°C on a 12 : 12 h light : dark cycle, and fed Romaine lettuce five times a week.

For primary cultures of isolated bag cell neurones, animals were anaesthetized by an injection of isotonic MgCl_2 (50% of body weight), the abdominal ganglion removed and treated with neutral protease (13.33 mg ml⁻¹; Roche Diagnostics, Indianapolis, IN, USA) for 18 h at 20–22°C, dissolved in tissue culture artificial sea water (tcASW) (composition (mM): 460 NaCl, 10.4 KCl, 11 CaCl₂, 55 MgCl₂, 15 Hepes, 1 mg ml⁻¹ glucose, 100 U ml⁻¹ penicillin, and 0.1 mg ml⁻¹ streptomycin, pH 7.8 with NaOH). The ganglion was then transferred to fresh tcASW for 1 h, after which time the bag cell neurone clusters were dissected from their surrounding connective tissue. Using a fire-polished Pasteur pipette and gentle trituration, neurones were dispersed in tcASW onto 35 mm \times 10 mm polystyrene tissue culture dishes (Corning, Corning, NY, USA). Cultures were maintained in tcASW in a 14°C incubator, and used for experimentation within 1–3 days. Salts were obtained from Fisher Scientific (Ottawa, ON, Canada), ICN (Aurora, OH, USA), or Sigma-Aldrich (St Louis, MO, USA).

Excised, patch-clamp recording

Single cation channel current was measured using an EPC-8 amplifier (HEKA Electronics, Mahone Bay, NS, Canada), and primarily the excised, inside-out patch-clamp method. Microelectrodes were pulled from 1.5 mm internal diameter, borosilicate glass capillaries (TW 150 F-4; World Precision Instruments, Sarasota, FL, USA) and were fire polished to a resistance of 2–8 M Ω when filled with normal artificial sea water (nASW) (composition as per tcASW but lacking glucose, penicillin, and streptomycin). To lower the root mean squared noise of the current signal, microelectrode capacitance was reduced by coating the shank and half of the shoulder with dental wax (Heraeus Kulzer, South Bend, IN, USA) under a dissecting microscope. Following excision, the cytoplasmic face was bathed with artificial intracellular saline (composition (mM): 500 potassium aspartate, 70 KCl, 1.2 MgCl₂, 10 Hepes, 11 glucose, 5 EGTA, 10 reduced glutathione, pH adjusted to 7.3 with KOH). In the majority of experiments, CaCl₂ was added for a free Ca^{2+} concentration of 1 μM . Some experiments were performed using intracellular saline with Ca^{2+} or Ba^{2+} concentrations ranging from 100 nM to 300 μM . Experiments involving Ba^{2+} required the substitution of CaCl₂ with BaCl₂. In all cases, the added and free Ca^{2+} and Ba^{2+} concentrations were calculated using the WebMaxC program (<http://www.stanford.edu/~cpatton/webmaxc/webmaxcE.htm>). In one set of experiments, single-channel current was measured using the excised, outside-out patch-clamp technique. Microelectrodes were filled with artificial intracellular saline containing 1 μM or 300 μM free Ca^{2+} . The extracellular face of excised, outside-out patches was exposed to nASW containing 11 mM Ca^{2+} or 11 mM Ba^{2+} . In all cases, current was low-pass filtered at 1 kHz using the EPC-8 Bessel filter and acquired at a sampling rate of 10 kHz using an IBM-compatible personal computer, a Digidata 1300 analog-to-digital converter (Axon Instruments, Union City, CA, USA), and the Clampex acquisition program of pCLAMP (version 8.0; Axon Instruments). Data were gathered at room temperature ($\sim 22^\circ\text{C}$) in 1–3 min intervals, typically while holding the patch at -60 mV.

Patch perfusion array, drug application and reagents

An eight-barrel perfusion array was constructed by tightly aligning borosilicate square tubing (outer diameter: 0.75 mm, internal diameter: 0.5 mm; VitroCom Inc., Mountain Lakes, NJ, USA) attached to one another using superglue. The section of the array that was submerged into the bath did not come in contact with superglue. The barrels at the opposite end of the array were fitted with silicone tubing (outer diameter: 3.3 mm, internal

diameter: 0.8 mm; Cole Parmer, Vernon Hills, IL, USA). Each of these perfusion lines was connected to a 5 ml syringe. Prior to experimentation, the entire perfusion system was rinsed with Sigmacote (SL-2; Sigma-Aldrich) and allowed to dry for at least 24 h. Gravitational flow was controlled by an alligator clip over the tubing and setting the level of the syringes to a fixed height. When the clip was released, the result was a flow of $\sim 1 \text{ ml min}^{-1}$. Any greater flow rate disturbed the patch and led to mechanical-based noise or seal failure. The perfusion system allowed patches to be moved from the mouth of one barrel to the next, permitting an almost instantaneous change in solutions at the face of the channel. During perfusion, the culture dish was gently drained as required using a plastic Pasteur pipette.

Drugs were made up as concentrated stock solutions and frozen at -30°C . They were introduced to the patch at the indicated working concentration, either with the perfusion array or by pipetting a small volume of stock solution into the culture dish. In the latter case, care was taken to pipette the stock near the side of the dish and as far away as possible from the patch at the tip of the microelectrode. In experiments examining the interplay of Ca²⁺ concentration and voltage dependence, TEA (Sigma-Aldrich) was added to nASW in the pipette to a final concentration of 20 mM in order to reduce outward currents through Ca²⁺-activated K⁺ channels. At or approaching 0 mV, these currents interfered with resolving inward current through the cation channel. Three calmodulin pharmacological inhibitors were employed to test the role of calmodulin as the cation channel Ca²⁺ sensor. Calmidazolium chloride (Calbiochem, San Diego, CA, USA) was dissolved in 100% ethanol for a stock solution of 14.5 mM. Calmidazolium (10 μM final) or its ethanol control (0.07% final) were perfused onto the cytoplasmic face of excised, inside-out patches. Similarly, *N*-(6-aminoethyl)-1-naphthalenesulphonamide HCl (W-5) (Calbiochem) was dissolved in 100% ethanol for a stock solution of 70 mM. W-5 (100 μM final) or its ethanol control (0.15% final) were also perfused onto the cytoplasmic face of excised, inside-out patches. Calmodulin-binding domain (CBD) (Calbiochem) was dissolved in sterile, double-distilled H₂O for a stock solution of 2.2 mM. For experiments, a small volume of CBD, 17 μl (50 μM final), was pipetted into a centre-well organ culture dish (VWR, Mississauga, ON, Canada) containing 750 μl of intracellular saline. Recording of cation channel current from excised, inside-out patches began following a short diffusion period of $\sim 1 \text{ min}$.

Calmodulin purification

Calmodulin was purified using repeated chromatography on phenyl-Sepharose from an *Escherichia coli* strain

(BL21) stably transformed with the expression plasmid (pCAM) coding for wild-type bovine calmodulin (accession number P62157). A sample of frozen *E. coli* cell stock was a gift from Dr A. S. Mak (Department of Biochemistry, Queen's University, Kingston, Ontario, Canada). The sample was cultured in 80 ml of LB broth with 100 $\mu\text{g ml}^{-1}$ ampicillin (Fisher) and grown overnight at 37°C with shaking at 250 r.p.m. The following day, 20 ml of the overnight culture was inoculated into 1 l of LB broth with 100 $\mu\text{g ml}^{-1}$ ampicillin and grown at 37°C , shaking at 250 r.p.m. until an OD600 of 0.8–1.1 was reached. The bacteria were then induced with 1 mM isopropyl- β -D-thiogalactoside (Fisher) at 30°C for 4 h. Cells were then spun down for 25 min at 600g at 4°C , the supernatant discarded, and the pellet frozen at -80°C overnight. On ice, cells were resuspended in 50 ml of buffer A (containing: 25 mM Tris-HCl pH 7.5, 1 mM DTT (Fisher), 0.02% NaN₃, and 0.1 mg ml⁻¹ phenylmethylsulphonyl fluoride (PMSF) (Sigma-Aldrich)). Cells were ruptured by sonicating the solution 5–10 times at 30 s intervals separated by 1 min rest periods, until the solution was visibly clearer and less viscous. The solution was then centrifuged at 17 500g (JA-20) for 40 min at 4°C , after which time the pellet was discarded and the supernatant centrifuged at 110 000g (Ti45) for 1 h at 4°C . CaCl₂ was added to a concentration of 2.5 mM to expose the hydrophobic regions of calmodulin, and stored overnight at 4°C . A disposable chromatography column (732 1010; Biorad, Hercules, CA, USA) was packed with 5 ml phenyl-Sepharose beads (Amersham, Piscataway, NJ, USA) and pre-equilibrated with 25 ml of H₂O and 25 ml of buffer B (containing: 25 mM Tris-HCl (pH 7.5) and 2.5 mM CaCl₂). The column was capped with parafilm and stored overnight at 4°C . At room temperature, the column was rinsed with 5 ml of buffer B. Extracts were mixed with phenyl-Sepharose beads in the column and left to sit for 30 min with gentle mixing every 5 min. The column was washed with 50 ml of buffer B, then washed with 100 ml of buffer C (containing: 50% buffer B and 0.5 M NaCl), and eluted with buffer E (containing: 25 mM Tris-HCl (pH 7.5), 0.5 M NaCl, 5 mM EGTA). Three different elutions of 5 ml were collected in separate tubes and tested for protein content using a protein assay kit (500-0006; Biorad). The second elution tube contained protein and was added to a 5 kDa cut-off ultrafreezable centricon (UFV2BCC10-5K; Millipore, Nepean, ON, Canada) to concentrate the calmodulin. The centricon was centrifuged at 400g at 4°C until 1 ml of buffer E remained, at which time it was rinsed with 5 ml of intracellular saline containing 10 μM free Ca²⁺. This step was repeated, and centrifugation continued until 1 ml of calmodulin in intracellular saline remained in the centricon. The absorbance of calmodulin (at 280 nm) was then tested with spectrophotometry, and combined with the extinction

coefficient of calmodulin (peptide property calculator; <http://www.basic.northwestern.edu/biotools/proteincalc.html>) to calculate calmodulin concentration. Aliquots (260 μM stock, 25 μl) were prepared and kept at -80°C prior to experimentation. During experiments, the stock calmodulin was diluted down to a final concentration of 3 μM by pipetting into a bath containing an excised, inside-out patch bathed in intracellular saline with 10 μM free Ca^{2+} . As a control, aliquots of stock calmodulin were boiled for 10 min prior to application.

As a test of calmodulin protein stability, a SDS-PAGE gel was run. From a working stock of 7.36 mg ml^{-1} , 1.5 μl (11 μg), 7.5 μl (55 μg), or 15 μl (110 μg) was added to a sample buffer (containing: 62.5 mM Tris-HCl pH 6.8 at 25°C , 2% (w/v) SDS, 10% glycerol, 0.01% (w/v) bromophenol blue and 42 mM DTT totalling a final volume of 30 μl). Samples and standards were boiled for about 5 min, and 20 μl of each loaded into a lane and allowed to run for ~ 4 h. By comparison to a broad-range protein marker (7701-S; New England Biolabs, Ipswich, MA, USA), the gel indicated that the purified protein was calmodulin ($\sim 17\ 000$ kDa) and that no degradation had occurred.

Data analysis

To determine channel open probability (P_o), events lists were made from data files using the half-amplitude threshold criterion (Colquhoun & Sigworth, 1995) of the Fetchan analysis program of pCLAMP. Fetchan was also used to generate all-points histograms for determining channel amplitude. For display in figures, all data were filtered to a final cut-off frequency of 500 Hz using the Fetchan digital Gaussian filter. The Pstat analysis program of pCLAMP was used to read events lists and determine P_o , either automatically or manually, using the formula:

$$P_o = (1 \times t_1 + 2 \times t_2 + \dots n \times t_n) / (N \times t_{\text{tot}})$$

where t = the amount of time that n channels are open, N = the number of channels in the patch, and t_{tot} = the time interval over which P_o is measured. The number of channels in the patch was determined by counting the number of unitary current levels, particularly at more positive voltages (typically -20 mV). Pstat was also used to determine the mean open- and closed-state current level by fitting all-points histograms with Gaussian functions using the least-squares method and a simplex search. Channel current amplitude was then calculated by subtracting the mean closed current level from the mean open current level at a given voltage.

The concentration–response curve was constructed using P_o values obtained at each concentration of Ca^{2+} or Ba^{2+} , which were normalized by dividing by the P_o at 300 μM Ca^{2+} , averaged, and plotted *versus* divalent concentration using Origin (version 7;

OriginLab Corporation, Northampton, MA, USA). The Ca^{2+} concentration–response curve was then fitted with a Hill function to yield the EC_{50} and Hill coefficient. The Ba^{2+} concentration–response curve could only be fitted by linear regression. To make P_o *versus* voltage relationships, P_o was first normalized to P_o at 0 mV and then plotted against patch holding potential using Origin. This relationship was then fitted with a Boltzmann function to derive the half-maximal voltage ($V_{0.5}$) and the slope factor (k), which is the change in voltage required to move the P_o e-fold. Channel current *versus* voltage relationships were produced in Origin by plotting channel-current amplitude against patch-holding potential, and single-channel conductance was then determined by linear regression. Predicted reversal potential was extrapolated from the Origin linear regression fit.

Statistical analysis

Data are presented as the mean \pm s.e.m. throughout. Statistical analysis was performed using Instat (version 3; GraphPad Software, San Diego, CA, USA). Student's t test (two-tailed or one-tailed, and paired or unpaired) was used to test whether the mean differed between two groups. A standard ANOVA with Dunnett's multiple comparisons test was used to test for differences between multiple means. The test for linear trend was used to determine if there was statistically significant linear trend in a series of multiple means. Analysis of outside-out recordings was based on a Ba^{2+} -induced percentage change in P_o or current amplitude. The P_o and current amplitude with Ca^{2+} at the extracellular face was considered to have a mean of zero, and the data with Ba^{2+} at the extracellular face were compared for a difference from that mean of zero using a two-tailed, one-sample t test. In all cases, data were considered significantly different if the P value was < 0.05 .

Results

The bag cell neurone cation channel is activated by Ca^{2+}

Cation channels were identified in excised, inside-out patches from cultured bag cell neurones by their conductance (25–30 pS; ~ 2 pA at -60 mV), voltage dependence of opening (an increase in P_o with depolarization), and absence of voltage-dependent inactivation. Many cation channels are regulated by Ca^{2+} , yet few Ca^{2+} concentration–response curves for neuronal cation channels are published. We perfused the cytoplasmic face of cation channel-containing patches with intracellular saline that had a free Ca^{2+} concentration

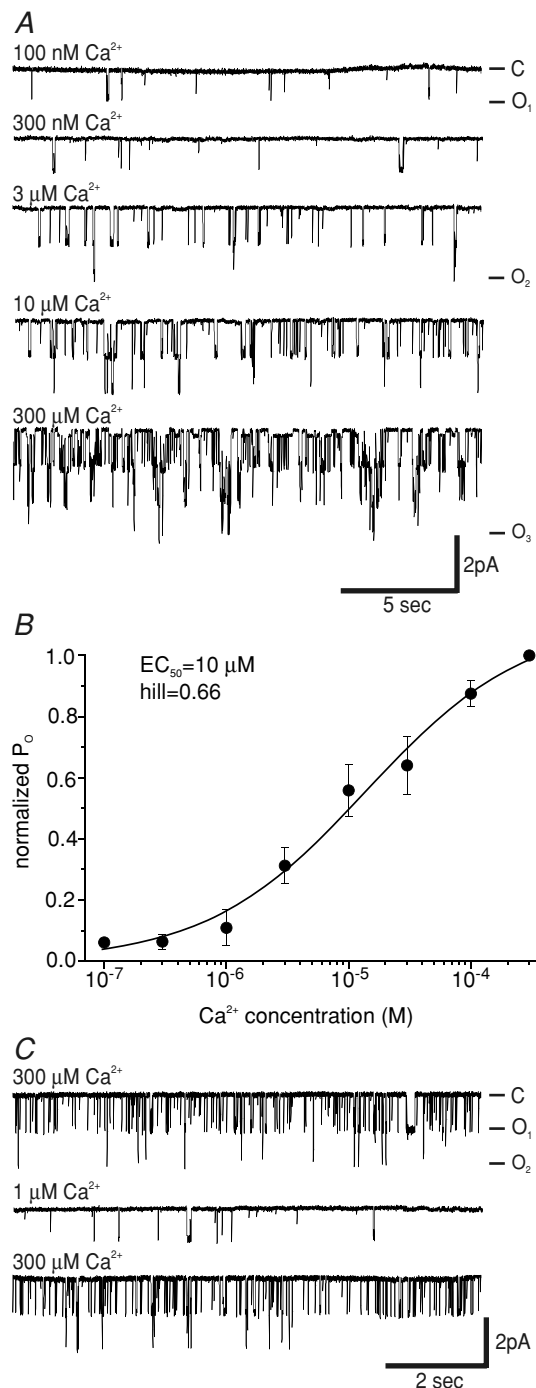


Figure 1. Concentration-dependent effects of Ca²⁺ on the cation channel

A, sample traces of cation channel activity recorded from an excised, inside-out patch held at -60 mV. Cation channel activity, seen as unitary inward current deflections of ~ 2 pA, steadily increases as the cytoplasmic face is perfused with intracellular saline containing 100 nM to 300 μ M Ca²⁺. The closed state is at the top of the trace and designated by C, while the open states are at the bottom and designated by O₁, O₂ and O₃. B, concentration–response of cation channel P_o exposed to a range of Ca²⁺ concentrations. All patches were exposed to 300 μ M Ca²⁺ ($n = 24$) with the remaining concentrations consisting of: 100 nM ($n = 6$), 300 nM ($n = 6$), 1 μ M ($n = 9$), 3 μ M ($n = 9$), 10 μ M ($n = 13$), 30 μ M ($n = 11$) and 100 μ M

ranging from 100 nM to 300 μ M (Fig. 1A). Upon excision, the patch was always initially perfused with intracellular saline containing 300 μ M Ca²⁺; subsequently, as many concentrations from within the range as possible were then delivered. Individual P_o values from a total of 24 patches exposed to some or all of the concentration range were normalized to 300 μ M Ca²⁺ and plotted versus Ca²⁺ concentration (Fig. 1B). Cation channel activity was maximal at 300 μ M Ca²⁺ and above (data not shown), and gradually diminished upon exposure to decreasing concentrations of free Ca²⁺ to a minimum, but still detectable level, in 100 nM Ca²⁺. The concentration–response curve was fitted with a Hill function, yielding an EC₅₀ of 10 ± 5 μ M Ca²⁺ and a Hill coefficient of 0.66 ± 0.1 . The response of the channel to the concentration of Ca²⁺ was independent of the order in which the Ca²⁺ concentrations were presented after the initial 300 μ M Ca²⁺. For a given channel, the P_o upon initial exposure to 300 μ M Ca²⁺ was very similar to a repeated exposure, even after application of any of the lower concentrations and vice versa (Fig. 1C). Thus, cation channel activity was reversible and highly dependent on cytoplasmic face Ca²⁺ concentration, confirming its Ca²⁺-dependent activation.

The voltage dependence of cation channel P_o is modulated by Ca²⁺

The voltage dependence of cation channel P_o is known to be modulated by Ca²⁺ in hamster vomeronasal sensory neurones (Liman, 2003) and membrane vesicles from placenta (Gonzalez-Perrett *et al.* 2002). Wilson *et al.* (1996) examined the effect of Ca²⁺ on the voltage dependence of the bag cell neurone cation channel, and suggested that increasing the cytoplasmic face Ca²⁺ from 100 nM to 1 μ M caused a hyperpolarizing shift in the P_o versus voltage curve. The present study examined the voltage dependence of bag cell neurone cation channel P_o as a function of 100 nM, 10 μ M, or 300 μ M cytoplasmic face Ca²⁺. The voltage dependence of the cation channel was maintained at all three Ca²⁺ levels such that P_o increased with depolarizing potentials. Figure 2A shows an example of this effect at 300 μ M Ca²⁺. When held at potentials positive to 0 mV, the cation channel current did not

($n = 11$). In three of these 24 cases, the patch was exposed to the entire concentration range (100 nM to 300 μ M). P_o was normalized to P_o at 300 μ M Ca²⁺. Data points fitted with a Hill function yield an EC₅₀ of 10 ± 5 μ M and a Hill coefficient of 0.66 ± 0.1 . C, sample traces of cation channel activity recorded from an excised, inside-out patch held at -60 mV. Upon exchange of the intracellular saline perfusing the cytoplasmic face from one containing 300 μ M Ca²⁺ to one with 100 nM, the activity decreases. However, this effect is completely reversible and the P_o reverts back to the prior level upon return to 300 μ M Ca²⁺.

reverse, but became unresolvable. This lack of reversal may be due to block by cytoplasmic face Mg^{2+} , as found in astrocyte (Chen & Simard, 2001) and TRPC5 (Obukhov & Nowycky, 2005) cation channels. Thus, despite not being an ideal standardization, P_o was normalized to P_o at 0 mV, which in turn revealed an apparent hyperpolarizing shift in voltage dependence without a change in sensitivity at 10 μM ($n=6$) or 300 μM Ca^{2+} ($n=9$) as compared to 100 nM Ca^{2+} ($n=5$) (Fig. 2B). The $V_{0.5}$ increased from -12 ± 0.8 mV in 100 nM Ca^{2+} to

-30 ± 0.5 mV or -27 ± 0.2 mV in 10 μM or 300 μM Ca^{2+} , without an appreciable change in the k (15 ± 0.7 versus 17 ± 0.4 versus 16 ± 0.2 in 100 nM versus 10 μM versus 300 μM Ca^{2+} , respectively). Overall, channel activity not only increased upon exposure to increasing Ca^{2+} levels, but as the membrane was depolarized, the increase in channel activity was further enhanced by the presence of 10 μM or 300 μM Ca^{2+} . Not surprisingly, linear regression analysis of current–voltage relationships in the three Ca^{2+} concentrations showed no change in the conductance or, as established by extrapolating beyond 0 mV, the reversal potential (data not shown).

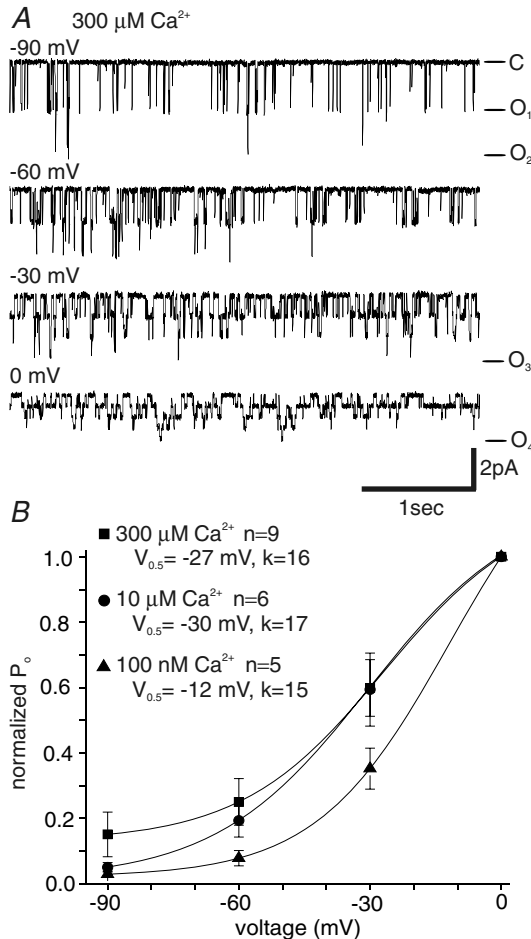


Figure 2. Interaction between Ca^{2+} and voltage dependence of the cation channel

A, sample traces of cation channel activity recorded from an excised, inside-out patch perfused with intracellular saline containing 300 μM Ca^{2+} and held at the indicated voltages. As the membrane potential is depolarized, channel activity increases. B, mean cation channel P_o normalized to P_o at 0 mV for each respective Ca^{2+} concentration and plotted against voltage. As given in the inset, points fitted with a Boltzmann function yield values for half-maximal activation ($V_{0.5}$) and slope factor (k). When Ca^{2+} is elevated from 100 nM to 10 μM , the voltage dependence shifts in the hyperpolarizing direction ($V_{0.5} = -12 \pm 0.8$ mV versus -30 ± 0.5 mV) without an appreciable alteration in sensitivity ($k = 15 \pm 0.7$ versus 17 ± 0.4); however, a further increase in Ca^{2+} to 300 μM does not cause any obvious additional change ($V_{0.5} = -27 \pm 0.2$ mV; $k = 16 \pm 0.2$).

The bag cell neurone cation channel is not sensitive to Ba^{2+}

The Ca^{2+} sensitivity of ion channels is mediated by Ca^{2+} binding directly to the channel or a channel-associated Ca^{2+} sensor (Hille, 2001; Levitan & Kaczmarek, 2001). The most versatile and ubiquitous Ca^{2+} sensor is calmodulin (Berridge *et al.* 2000), and it has been implicated in mediating the Ca^{2+} sensitivity of numerous ion channels (Levitan, 1999). To initially test this, we used a method first carried out on small-conductance Ca^{2+} -activated K^+ channels (Cao & Houamed, 1999); namely, Ba^{2+} was substituted for Ca^{2+} and perfused on the cytoplasmic face of the cation channel. The rationale is based on Ba^{2+} binding/activating calmodulin poorly because it is a weak substitute for Ca^{2+} at the EF-hand motifs (Haiech *et al.* 1981; Chao *et al.* 1984; Wang, 1985; Ozawa *et al.* 1999). Therefore, if calmodulin mediates Ca^{2+} sensitivity of the cation channel, replacing Ca^{2+} with Ba^{2+} would result in a failure to activate the channel in a concentration-dependent fashion. Cation channel-containing patches were initially exposed to intracellular saline containing 300 μM Ca^{2+} , and then subsequently perfused with intracellular saline containing Ba^{2+} ranging in concentration from 100 nM to 300 μM ($n=6$). Cation channel P_o was dramatically reduced upon exposure to Ba^{2+} and remained relatively unchanged throughout the concentration range (Fig. 3). Overall, the cation channel showed very little, if any, sensitivity to Ba^{2+} , suggesting a possible involvement of calmodulin as the sensor mediating Ca^{2+} dependence of channel activity.

Ba^{2+} as a charge carrier reduces cation channel activity

For voltage-gated Ca^{2+} channels, Ca^{2+} entry in turn inactivates the channel through associated calmodulin, and this can be prevented by substituting Ba^{2+} for Ca^{2+} as a charge carrier (Zuhlke *et al.* 1999). To examine if Ca^{2+} entry through the cation channel also serves as a regulator, patches were excised from bag cell neurones in

the outside-out configuration, and the extracellular face of the channel was perfused with nASW containing 11 mM Ca²⁺ followed by ASW with Ba²⁺ substituted for Ca²⁺. The pipette, which bathed the cytoplasmic face, contained intracellular saline with either 1 μ M or 300 μ M Ca²⁺ ($n = 4$ and 4) (Fig. 4A and B). In agreement with Ba²⁺ permeating the cation channel as a superior charge carrier, following perfusion with Ba²⁺ the current amplitude increased by $\sim 18\%$ with 1 μ M Ca²⁺, and $\sim 15\%$ with 300 μ M Ca²⁺ in the pipette (Fig. 4C). Wilson *et al.* (1996) reported that the relative monovalent cation permeability of the channel was $K^+ \approx Na^+ \gg Tris > NMDG$; moreover, consistent with Ca²⁺ permeability and our data on enhanced current amplitude under external Ba²⁺, they showed that replacing external Ca²⁺ with Ba²⁺ caused the conductance to increase from 29 pS to 36 pS. However, Wilson *et al.* (1996) did not report at all regarding the effect of external Ba²⁺ on P_o . We found that Ba²⁺ perfusion produced an $\sim 70\%$ and $\sim 50\%$ decrease in P_o with 1 μ M and 300 μ M Ca²⁺ in the pipette, respectively (Fig. 4C). This drop in P_o is probably due to a loss of Ca²⁺ activation. Changes to both current amplitude and P_o with either 1 μ M or 300 μ M Ca²⁺ in the pipette were statistically significant, and suggest that Ca²⁺ influx through the channel itself may be a source of Ca²⁺ activation.

Pharmacological block of calmodulin reduces cation channel activity

In those cases where calmodulin is the sensor mediating Ca²⁺-dependent channel regulation of ion channels, calmodulin antagonists often inhibit the effects of Ca²⁺ on channel function (Krupp *et al.* 1999; Michikawa *et al.* 1999; Bobkov & Ache, 2003; Moreau *et al.* 2005). Calmidazolium chloride is a potent, specific, and widely effective organic antagonist that inhibits many calmodulin-activated proteins (Van Belle, 1981; Gietzen *et al.* 1982; DeRiemer *et al.* 1985). When cation channels excised from bag cell neurones were perfused with intracellular saline containing 10 μ M calmidazolium and 1 μ M Ca²⁺, the P_o decreased ($n = 5$) (Fig. 5A). The antagonizing effect of calmidazolium on cation channel activity was also apparent at a cytoplasmic face Ca²⁺ concentration of 10 μ M or 300 μ M ($n = 6$ and 6) (Fig. 5B and C). When the cytoplasmic face of excised patches was exposed to ethanol, the vehicle for calmidazolium, cation channel activity decreased by no more than 30%, regardless of the Ca²⁺ concentration ($n = 5, 5$ and 5) (Fig. 5D). Compared to parallel ethanol controls, 10 μ M calmidazolium significantly reduced channel P_o by $\sim 60\%$ and 70% in 1 μ M and 10 μ M, respectively (Fig. 5E). The concentration dependence of calmidazolium was demonstrated by applying additional concentrations in the presence of 300 μ M Ca²⁺. At 3 μ M and 30 μ M ($n = 4$

and 4), calmidazolium caused lower ($\sim 45\%$) and higher ($\sim 90\%$) reductions in channel P_o than that produced by 10 μ M ($\sim 75\%$) (Fig. 5E).

DeRiemer *et al.* (1985) found that 50 μ M of the chloride-deficient calmodulin antagonist W-5 had no effect on the initiation of an afterdischarge in intact bag cell neurone clusters. In keeping with that prior negative result, when 100 μ M W-5 was tested on the cation channel

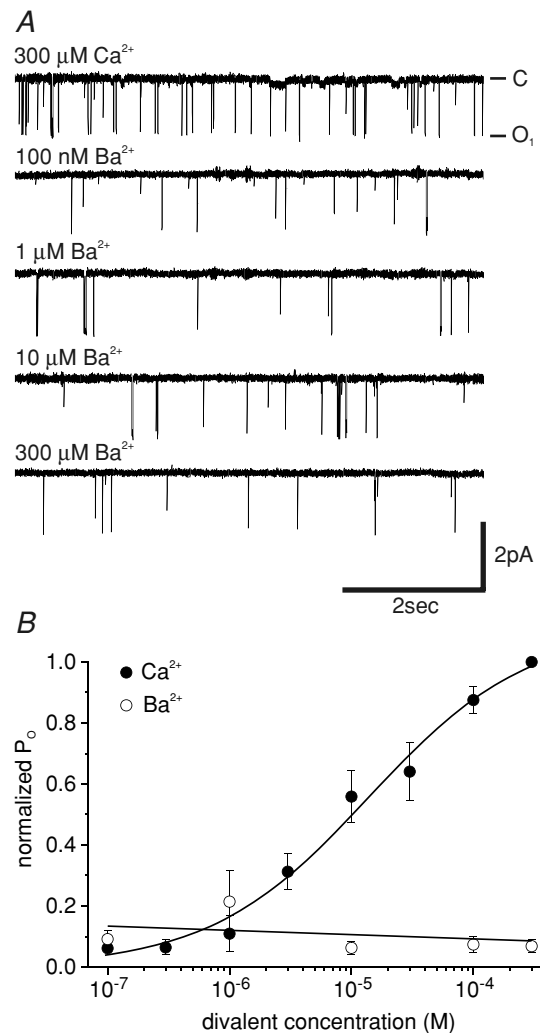


Figure 3. Lack of effect of Ba²⁺ on cation channel activity

A, sample traces of cation channel activity recorded at -60 mV from an excised, inside-out patch. The cytoplasmic face was perfused with intracellular saline with 300 μ M Ca²⁺ followed by intracellular saline with Ba²⁺ substituted for Ca²⁺ at concentrations ranging from 100 nM to 300 μ M. The Ba²⁺ intracellular saline contained no added Ca²⁺. Upon exchange to Ba²⁺, the P_o decreases and remains unchanged regardless of the concentration of subsequently applied Ba²⁺. B, summary of mean cation channel P_o after Ba²⁺ perfusion compared to that of Ca²⁺. P_o was normalized to P_o at 300 μ M Ca²⁺ (perfused onto each patch at the start of the experiment prior to the introduction of Ba²⁺) (○, $n = 6$). The points could only be fitted with a linear regression function. For comparison, the concentration–response curve for Ca²⁺ from Fig. 1B is replotted here (●).

it did not reduce P_o during perfusion with intracellular saline containing $300 \mu\text{M}$ Ca^{2+} ($n = 5$) (Fig. 5E). Due to its ineffectiveness at $300 \mu\text{M}$ Ca^{2+} , W-5 was not tested with intracellular saline containing $1 \mu\text{M}$ or $10 \mu\text{M}$ Ca^{2+} .

A synthetic peptide inhibitor of calmodulin, known as CBD and corresponding to residues 290–309 of the Ca^{2+} -calmodulin-dependent kinase regulatory domain, is highly effective at impairing calmodulin-mediated Ca^{2+} processes (Payne *et al.* 1988). This peptide is a very specific calmodulin antagonist and a reliable indicator

of calmodulin being involved in a process. The cytoplasmic face of excised, inside-out patches containing cation channels was exposed to $50 \mu\text{M}$ CBD added to intracellular saline containing $1 \mu\text{M}$, $10 \mu\text{M}$ and $300 \mu\text{M}$ Ca^{2+} ($n = 7, 6$ and 6) (Fig. 6A–C). CBD was manually added to the bath and allowed to diffuse for 1 min prior to a 5 min recording period. For controls, water (the vehicle) was initially employed, and it produced no change in cation channel activity ($n = 2$, data not shown). Subsequently, timed controls were used for analysis and can be described

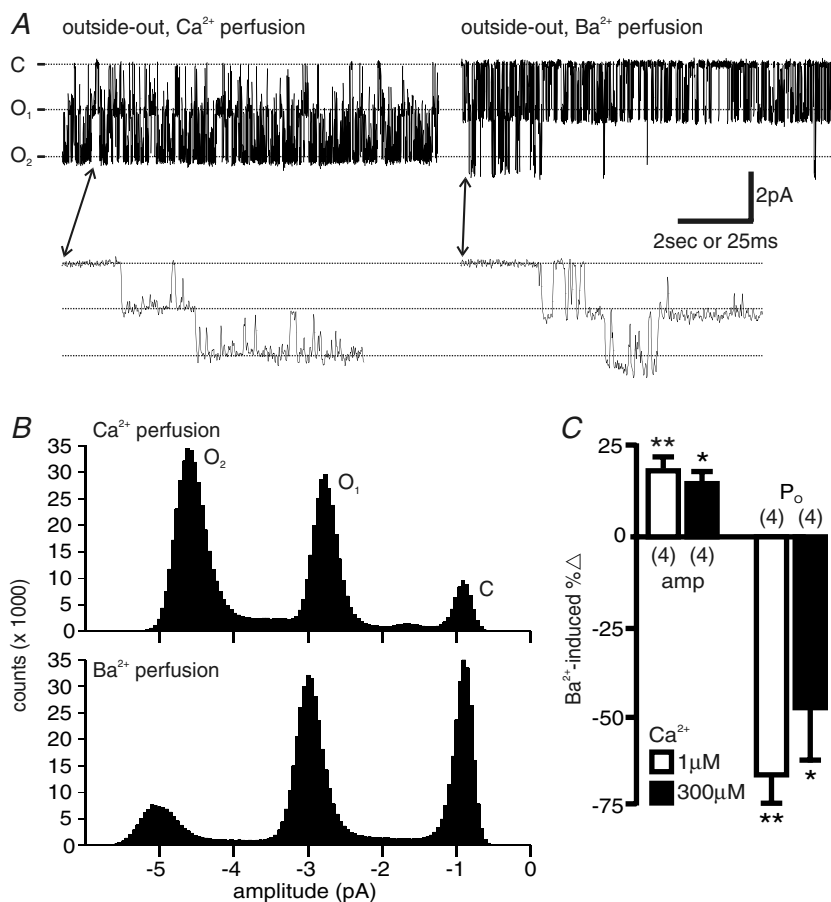


Figure 4. Extracellular Ba^{2+} decreases cation channel P_o and increases amplitude

A, sample traces recorded from an excised, outside-out patch held at -60 mV. The cytoplasmic face is exposed to intracellular saline (in the pipette) containing $300 \mu\text{M}$ Ca^{2+} , and upon excision the extracellular face is perfused with ASW (in the bath) containing 11 mM Ca^{2+} or 11 mM Ba^{2+} . Upper panel, replacement of Ca^{2+} with Ba^{2+} at the extracellular face results in both an increased channel amplitude and a lowering of P_o . The closed and two open current levels are indicated by dotted lines. The 2 s time base applies. Lower panel, 100 ms portion of cation channel activity during both Ca^{2+} and Ba^{2+} perfusion taken from the upper panel at times indicated by arrows. The dotted lines again show the increase in current amplitude when Ba^{2+} replaces Ca^{2+} . The 25 ms time base applies. B, all-points histograms from the outside-out patch shown in A. The closed (C) and two open (O_1 , O_2) current levels are denoted just to the right of their corresponding peaks. An increase in current amplitude with Ba^{2+} versus Ca^{2+} application is evident by the left shift in both of the open state peaks. C, summary of Ba^{2+} -induced percentage changes in P_o and current amplitude from outside-out patches. Ba^{2+} -induced percentage changes are compared to a mean of zero using a two-tailed, one-sample *t* test. When recorded with intracellular saline containing either $1 \mu\text{M}$ or $300 \mu\text{M}$ Ca^{2+} , the P_o and current amplitude (amp) are significantly reduced and enhanced, respectively, by the perfusion of Ba^{2+} ($*P < 0.05$ or $**P < 0.01$). For this and all subsequent bar graphs, the *n* values are given within, just below, or just above a given bar.

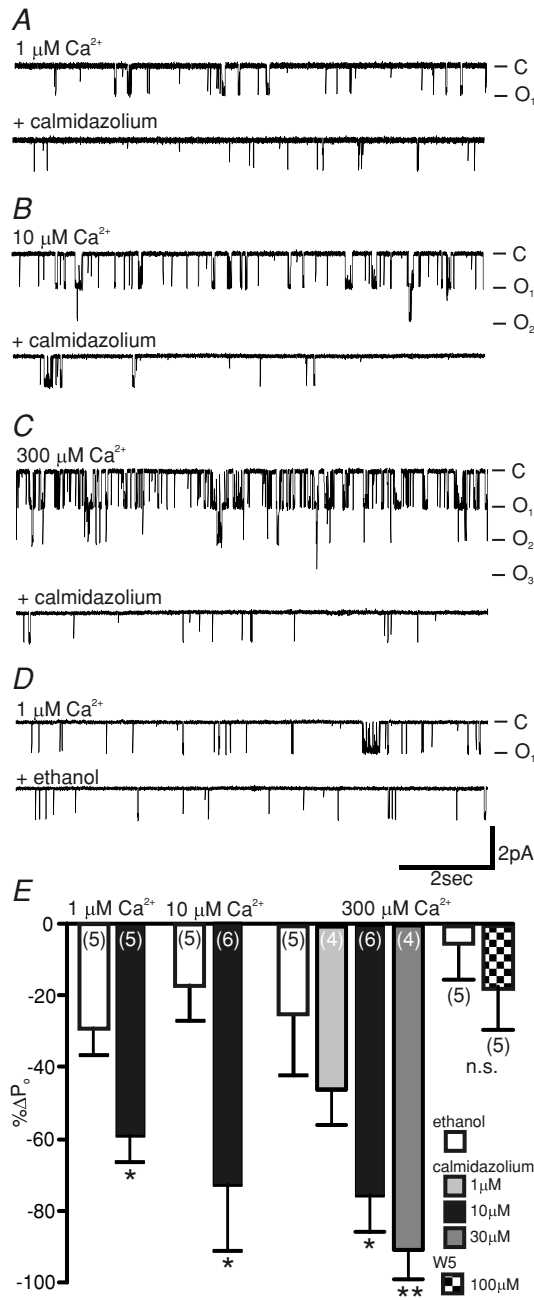


Figure 5. A calmodulin inhibitor decreases cation channel P_o
 A–C, sample traces, before and after 10 μM calmidazolium, of cation channel activity in an excised, inside-out patch held at -60 mV with the cytoplasmic face bathed in intracellular saline containing 1 μM , 10 μM , or 300 μM Ca²⁺. At each Ca²⁺ concentration, there is a clear and obvious decrease in P_o upon addition of calmidazolium. D, sample traces before and after 0.15% ethanol (the vehicle), of cation channel activity in a patch held at -60 mV with the cytoplasmic face bathed in intracellular saline containing 1 μM Ca²⁺. Ethanol causes only a modest reduction in P_o . E, a summary of the mean percentage change in cation channel P_o showing the effect of ethanol versus calmidazolium or W-5-treated patches in intracellular saline containing 1 μM , 10 μM , or 300 μM Ca²⁺. A two-tailed, unpaired t test comparing separate ethanol controls to 10 μM calmidazolium shows that the decrease in P_o reaches significance in the presence of either

as the percentage change in cation channel activity between the first and second half of the control period prior to the addition of CBD. Compared to timed controls, 50 μM CBD caused a significant decline in cation channel P_o of $\sim 20\%$, 40% , and 65% in 1 μM , 10 μM , and 300 μM Ca²⁺, respectively (Fig. 6D). Collectively, the antagonizing effects of pharmacological blockers of calmodulin support the role of calmodulin in Ca²⁺-dependent cation channel activation.

Purified bovine calmodulin increases cation channel activity

The application of exogenous calmodulin to Ca²⁺-sensitive ion channels is a widely practised method to assess possible modulation by this protein (Liu *et al.* 1994; Zhang *et al.* 1998; Krupp *et al.* 1999; Zuhlke *et al.* 1999; Rycroft & Gibb, 2004; Bradley *et al.* 2004). Excised, inside-out patches containing cation channels were bathed in 10 μM intracellular Ca²⁺ and exposed to 3 μM of either intact or boiled/denatured purified bovine calmodulin. Calmodulin was used in the presence of a Ca²⁺ concentration that led to a 50% activation of the cation channel, i.e. 10 μM . Exogenous calmodulin caused a significant, $\sim 60\%$ increase in cation channel P_o (Fig. 7A and C), whereas when the protein was heat-inactivated it induced a moderate, $\sim 20\%$ reduction in P_o (Fig. 7B and C). Overall, 10 μM Ca²⁺ was sufficient to activate 3 μM of added calmodulin to cause an increase in bag cell neurone cation channel activity.

Discussion

Ca²⁺-activated, non-selective cation channels are essential to the control of neuronal excitability and the generation of depolarizing afterpotentials, plateau potentials, or bursting (Kramer & Zucker, 1985; Swandulla & Lux, 1985; Partridge & Swandulla, 1988; Partridge *et al.* 1994; Zhang *et al.* 1995; Congar *et al.* 1997; Haj-Dahmane & Andrade, 1997; Rekling & Feldman, 1997; Morisset & Nagy, 1999; Egorov *et al.* 2002). In *Aplysia* bag cell neurones, a cation channel provides the depolarizing drive for an afterdischarge that triggers egg-laying behaviour (Conn & Kaczmarek, 1989; Wilson *et al.* 1996). A prior report found that elevating cytoplasmic face Ca²⁺ from

1 μM or 10 μM Ca²⁺ ($*P < 0.05$). An ANOVA followed by Dunnett's multiple comparisons test shows that 10 and 30 μM calmidazolium produce significant and concentration-dependent decreases in P_o in the presence of 300 μM Ca²⁺ ($*P < 0.05$ or $**P < 0.01$). A test for linear trend among the 300 μM Ca²⁺ points also shows that there is a significant linear trend, i.e. a negative slope with increasing calmidazolium concentration ($P < 0.005$). In 300 μM Ca²⁺, a one-tailed, unpaired t test finds no significant (n.s.) difference between W-5-treated patches and ethanol controls.

100 nM to 1 μM increased channel activity threefold (Wilson *et al.* 1996). We now show that the cation channel is indeed Ca^{2+} activated, through what appears to be a close, physical association with calmodulin.

Ca^{2+} activation is a defining characteristic of many cation channels. First described in cardiac Purkinje

fibres (Kass *et al.* 1978), this process has been studied at the single-channel level in various cells, including cardiomyocytes (Colquhoun *et al.* 1981; Guinamard *et al.* 2004), epithelia (Miyashita *et al.* 2001), kidney cells (Gonzalez-Perrett *et al.* 2002), hair cells (Van den Abbeele *et al.* 1994) neuroblastoma (Yellen, 1982), sensory neurones (Razani-Boroujerdi & Partridge, 1993; Cho *et al.* 2003; Liman, 2003) and *Helix* neurones (Partridge & Swandulla, 1987). Ca^{2+} activation of the bag cell neurone cation channel has an EC_{50} of 10 μM and peaks at 300 μM . Although cytoplasmic Ca^{2+} rarely exceeds 1 μM in spiking bag cell neurones (Fisher *et al.* 1994; Magoski *et al.* 2000), evidence from squid shows that, at the plasma membrane, the concentration in a Ca^{2+} channel microdomain can be 200–300 μM (Llinas *et al.* 1992). Also, depending on the distance from the pore, the nanodomain for single Ca^{2+} channels is 5–50 μM (Smith & Augustine, 1988; Neher, 1998). Thus, Ca^{2+} channels opened during the after-discharge would provide a substantial, near-membrane concentration of Ca^{2+} to the cation channel. In addition, release from intracellular stores would be a source of Ca^{2+} for cation channel activation (Fink *et al.* 1988; Magoski *et al.* 2000).

Both Wilson *et al.* (1996) and the present study provide evidence that the bag cell neurone cation channel is Ca^{2+} permeable. We also now show that substituting Ba^{2+} for Ca^{2+} as an extracellular charge carrier decreased channel P_o . Given that Ba^{2+} activates the channel poorly, this suggests that Ca^{2+} influx through the cation channel itself provides a degree of stimulation. In general, for those Ca^{2+} -activated, non-selective cation channels that are Ca^{2+} permeable, the intrinsically higher Ca^{2+} concentrations at the channel mouth may act as a regulator (Lan *et al.* 1996; Zitt *et al.* 1997; Strubing *et al.* 2001; Lambers *et al.* 2004). The result of Ba^{2+} permeation reducing bag cell neurone cation channel activity is, to our knowledge, some of the first evidence supporting such a mechanism. Conversely, a number of additional cation channels, such as TRPM4 and TRPM5, show little or no Ca^{2+} permeability and require other sources of Ca^{2+} influx or release for activation (Yellen, 1982; Chen & Simard, 2001; Miyashita *et al.* 2001; Launay *et al.* 2002; Cho *et al.* 2003; Liman, 2003; Prawitt *et al.* 2003; Guinamard *et al.* 2004).

Comparing the EC_{50} and Hill coefficient values of the bag cell neurone channel (10 μM and 0.66) to other cation channels reveals both similarities and differences, e.g. 460 nM and 0.49 in chick sensory neurones (Razani-Boroujerdi & Partridge, 1993), 510 μM and 2.1 in vomeronasal neurones (Liman, 2003), 774 μM and 0.97 in rat sensory neurones (Cho *et al.* 2003), or ~ 10 μM in cochlear hair cells (Van den Abbeele *et al.* 1994). The EC_{50} of the non-neuronal TRPM4b has been reported as 400 nM (Launay *et al.* 2002) or 15 μM (Nilius *et al.* 2005), while TRPM5, which probably plays a role in taste

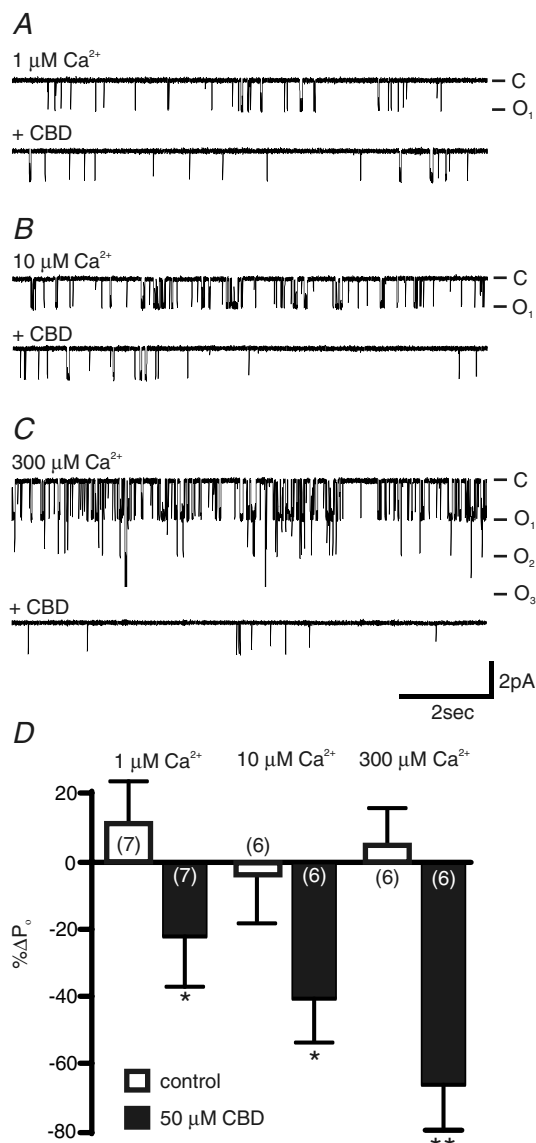


Figure 6. Calmodulin-binding domain inhibitor peptide (CBD) decreases cation channel P_o

A–C, sample traces of cation channel activity, before and after addition of 50 μM CBD, recorded from excised, inside-out patches held at -60 mV and bathed with intracellular saline containing 1 μM , 10 μM , or 300 μM Ca^{2+} . In each case, the delivery of CBD markedly lowers the P_o . D, a summary of the mean percentage change in P_o between timed controls and CBD-treated preparations. Timed controls are expressed as the percentage change between the first and second half of the control period. Comparisons using a one-tailed, paired t test show that the reduction in P_o during the CBD treatment period produces means that are significantly different from timed controls at 1 μM or 10 μM Ca^{2+} (* $P < 0.05$) and 300 μM Ca^{2+} (** $P < 0.01$).

transduction, has an EC₅₀ of either 840 nM or 21 μM, with a Hill coefficient of either 5.0 or 2.4 (Prawitt *et al.* 2003; Liu & Liman, 2003). A significant proportion of these EC₅₀ values are, like the bag cell neurone cation channel, in the micromolar range. In addition, the Hill coefficient of less than one for either the bag cell or chick sensory neurone channels suggests negative cooperativity. Perhaps initial Ca²⁺ binding lowers the affinity for additional binding, or Ca²⁺ may partially block the channels at higher concentrations. A Hill coefficient of 1.0, such as for rat sensory neurones, indicates competitive Ca²⁺ binding to a single site on the channel. Regarding the affinity of Ca²⁺ for calmodulin alone, in the absence of an effector protein such as a channel, Haiech *et al.* (1981) reported EC₅₀s of ~4 and ~7 μM in 100 and 200 mM KCl, respectively, for ⁴⁵Ca²⁺ binding to sheep calmodulin.

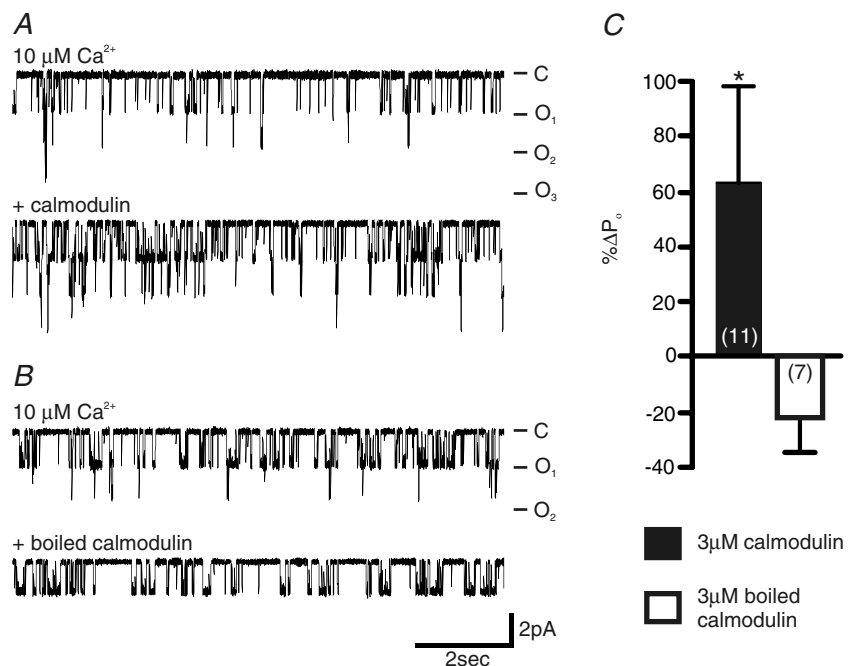
Some cation channels are voltage dependent, including those from cardiomyocytes (Guinamard *et al.* 2004), epithelia (Miyashita *et al.* 2001), superchiasmatic neurones (Kononenko *et al.* 2004), pyramidal neurones (Alzheimer, 1994), and vomeronasal neurones (Liman, 2003). For the bag cell neurone cation channel, activity is steadily enhanced at potentials positive to -60 mV; moreover, when Ca²⁺ is increased from 100 nM to 10 μM or 300 μM, the V_{0.5} shifts from -12 mV to ~-30 mV, with little change in *k* (~16 throughout). This is consistent with Wilson *et al.* (1996), who intimated that the P_o versus voltage curve shifted to the left when Ca²⁺ was increased from 100 nM to 1 μM. An interdependence of Ca²⁺ and voltage activation has also been observed for cation channels from vomeronasal neurones (Liman, 2003), astrocytes (Chen & Simard, 2001), and endothelia (Csanady &

Adam-Vizi, 2003), although for TRPM4b the V_{0.5} and *k* (+32 mV and 9) do not change overall when Ca²⁺ is altered (Nilius *et al.* 2003). In the case of the bag cell neurone cation channel, Ca²⁺ may not only act as a ligand by increasing P_o in a concentration-dependent manner, but could further augment activity by moving voltage dependence to more hyperpolarized potentials. During the afterdischarge, action potential firing occurs from a membrane potential of -20 to -40 mV (Conn & Kaczmarek, 1989), a range that readily accommodates the V_{0.5} (~-30 mV) of the cation channel in high Ca²⁺. However, such postulations are made knowing that the high-Ca²⁺-induced shift may be ostensible, given that P_o values in the present study were determined only for a limited range of voltages.

If cation channel Ca²⁺ activation is due to a channel-associated Ca²⁺ sensor, rather than Ca²⁺ binding directly to the channel, calmodulin is a good candidate. A ubiquitous Ca²⁺ sensor, calmodulin, mediates the Ca²⁺-dependent properties of numerous ion channels, including gating of small- and intermediate-conductance Ca²⁺-activated K⁺ channels (Xia *et al.* 1998; Levitan, 1999), activation of ryanodine receptors (Saimi & Kung, 2002), inactivation and facilitation of L-type Ca²⁺ channels (Zuhlke *et al.* 1999), as well as inhibition of CNG channels (Liu *et al.* 1994; Bradley *et al.* 2004), NMDA receptors (Zhang *et al.* 1998; Rycroft & Gibb, 2004), and IP₃ receptors (Michikawa *et al.* 1999). For the bag cell neurone cation channel, the P_o shows no concentration response to Ba²⁺, a metal that binds/activates calmodulin poorly (Haiech *et al.* 1981; Chao *et al.* 1984; Wang, 1985; Ozawa *et al.* 1999). Thus, as with Ca²⁺-activated K⁺ channels

Figure 7. Exogenous calmodulin increases cation channel P_o

A, sample traces of cation channel activity recorded from an excised, inside-out patch held at -60 mV and bathed in intracellular saline containing 10 μM Ca²⁺, before and after addition of 3 μM purified bovine calmodulin. The introduction of calmodulin robustly elevates cation channel P_o. **B**, sample traces of cation channel activity recorded from an excised, inside-out patch held at -60 mV and bathed in intracellular saline containing 10 μM Ca²⁺ before and after addition of 3 μM boiled calmodulin. Heat inactivation renders calmodulin modestly inhibitory. **C**, a comparison of the mean percentage change in P_o between excised inside-out patches treated with 3 μM calmodulin versus boiled calmodulin. A two-tailed, unpaired *t* test shows that the increase in cation channel P_o is significantly different following calmodulin administration compared to patches treated with boiled protein (**P* < 0.05).



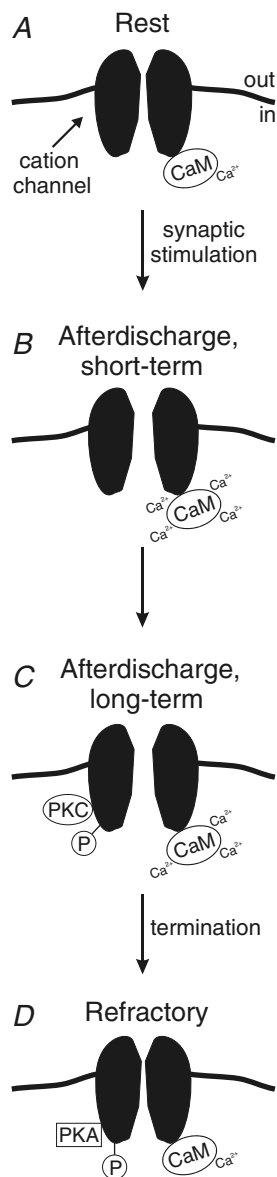


Figure 8. A complex of interchanging proteins regulates the cation channel during the afterdischarge

A, at rest, calmodulin (CaM) is associated with the cation channel, but activity is minimal due to the presence of low intracellular Ca^{2+} . Channel P_o is indicated by the width of the 'pore' in the illustration. B, following synaptic stimulation, an increase in intracellular Ca^{2+} activates the cation channel over the short term, as the afterdischarge begins (Wilson *et al.* 1996; present study). C, later in the afterdischarge, Ca^{2+} continues to activate the cation channel along with maintained upregulation provided by the simultaneous association of stimulatory PKC (Wilson *et al.* 1998; Magoski *et al.* 2002). D, upon termination of the afterdischarge, intracellular Ca^{2+} falls with the cessation of action potential firing. Either as a consequence of refractoriness, or as a mechanism contributing to refractoriness, inhibitory PKA is exchanged with PKC to downregulate the cation channel (Magoski, 2004; Magoski & Kaczmarek, 2005). During the refractory period, cation channel activity and bag cell neurone excitability are maintained at lowered levels, thus preventing the generation of additional afterdischarges which could disrupt ongoing egg-laying behaviour.

(Cao & Houamed, 1999) and Ca^{2+} channels (Zuhlke *et al.* 1999), the failure of Ba^{2+} to mimic Ca^{2+} suggests that calmodulin may be the cation channel Ca^{2+} sensor.

Calmodulin inhibitors have also been used to implicate calmodulin in channel regulation, e.g. 5–100 μM calmidazolium inhibits Ca^{2+} -dependent facilitation and inactivation of Ca^{2+} release-activated Ca^{2+} channels (Moreau *et al.* 2005), as well as the Ca^{2+} sensitivity of a Na^+ -activated cation channel in lobster olfactory neurones (Bobkov & Ache, 2003) and the *Drosophila* TRPL cation channel expressed in oocytes (Lan *et al.* 1996). Moreover, 10 μM calmidazolium strongly inhibits both *Aplysia* CNS Ca^{2+} -calmodulin-dependent kinase and the ability of bag cell neurones to fire an afterdischarge (DeRiemer *et al.* 1984, 1985). Depending on the added calmodulin concentration, calmidazolium maximally inhibits brain phosphodiesterase and blood cell Ca^{2+} -ATPase in the range of 100 nM to 3 μM (Van Belle, 1981). For phosphorylase kinase, a protein that incorporates calmodulin as a subunit, maximal inhibition requires more than 10 μM (Van Belle, 1981). Cation channel activity after exposure to 10 μM calmidazolium in 1 μM , 10 μM and 300 μM Ca^{2+} , was reminiscent of that in 100 nM Ca^{2+} . Regarding CBD, it was first shown to inhibit Ca^{2+} -calmodulin-dependent kinase II and phosphodiesterase by preventing calmodulin-enzyme binding (Payne *et al.* 1988). In addition, 20–25 μM CBD inhibits Ca^{2+} -dependent inactivation of NMDA (Krupp *et al.* 1999) or IP_3 receptors (Michikawa *et al.* 1999). Accordingly, we found that 50 μM CBD reduced bag cell neurone cation channel activity at 1 μM , 10 μM and 300 μM Ca^{2+} . This again indicates that, rather than Ca^{2+} binding directly to the channel, closely associated calmodulin acts as a Ca^{2+} sensor.

A role for calmodulin in cation channel Ca^{2+} sensitivity was further confirmed by our observation that 3 μM bovine calmodulin, in 10 μM Ca^{2+} , increased P_o . Bovine calmodulin readily activates various *Aplysia* proteins, including Ca^{2+} -calmodulin-dependent kinase (~500 nM calmodulin with 500 μM Ca^{2+}) (DeRiemer *et al.* 1984), adenylate cyclase (3 μM calmodulin with 3 μM Ca^{2+}) (Abrams *et al.* 1991), and twitchin (100 nM calmodulin with 1 mM Ca^{2+}) (Heierhorst *et al.* 1994). The effectiveness of exogenous calmodulin appears to depend on the combined protein and Ca^{2+} concentration. This is also apparent for exogenous calmodulin-mediated inhibition of CNG channels (500 nM calmodulin with 100 nM Ca^{2+}) (Bradley *et al.* 2004), NMDA receptors (100 nM calmodulin with 100 μM Ca^{2+}) (Krupp *et al.* 1999), and IP_3 receptors (20 μM calmodulin with 200 μM Ca^{2+}) (Michikawa *et al.* 1999), as well as enhancement of non-neuronal TRPM4b (10 μM calmodulin with 100 μM Ca^{2+}) (Nilius *et al.* 2005) and TRPM5 (10 μM calmodulin with 5–7 μM Ca^{2+}) (Ordaz *et al.* 2005). Interestingly, when any of the TRPM2, TRPM4b, TRPV5, or TRPV6

cation channels were coexpressed with a calmodulin mutant whose Ca²⁺-binding sites are impaired, the current was decreased (Lambers *et al.* 2004; Nilius *et al.* 2005; Tong *et al.* 2006). For both the bag cell neurone cation channel and others, exogenous calmodulin may displace endogenous calmodulin and/or bind to unoccupied calmodulin-binding sites.

In the bag cell neurones, intracellular Ca²⁺ rises rapidly upon synaptic stimulation, possibly due to release from intracellular stores (Fink *et al.* 1988). When the after-discharge begins, there is a second elevation due to activation of voltage-gated Ca²⁺ channels (Fisher *et al.* 1994). We propose that intracellular Ca²⁺ binds to cation channel-associated calmodulin to promote channel activation and the afterdischarge. Calmodulin appears to be one of several, closely associated regulatory proteins that are in a complex with the cation channel. In addition to Ca²⁺ activation, the P_o of the cation channel is also increased by closely associated protein kinase C (PKC) (Wilson *et al.* 1998; Magoski *et al.* 2002) or decreased by closely associated protein kinase A (PKA) (Magoski, 2004). These kinases can reconfigure depending on bag cell neurone excitability or activity levels. During the afterdischarge, stimulatory PKC is channel associated, while inhibitory PKA is present through the refractory period (Magoski & Kaczmarek, 2005). Calmodulin, which presumably is always present, would allow Ca²⁺ to influence cation channel activity in a graded fashion during the afterdischarge, with PKC maintaining spiking, and PKA then contributing to refractoriness (Fig. 8). Overall, this complex of regulatory proteins determines cation channel function and fundamentally affects species propagation.

In summary, we provide the first evidence that Ca²⁺ activation of a native, neuronal cation channel is mediated by closely associated calmodulin. Given the similarities between the bag cell neurone channel and other cation channels, calmodulin probably mediates Ca²⁺ sensitivity in many versions of this conductance. This crucial aspect of gating is central to the influence of these channels over neuronal excitability, activity and behaviour.

References

- Abrams TW, Karl KA & Kandel ER (1991). Biochemical studies of stimulus convergence during classical conditioning in *Aplysia*: dual regulation of adenylate cyclase by Ca²⁺/Calmodulin and transmitter. *J Neurosci* **11**, 2655–2665.
- Alzheimer C (1994). A novel voltage-dependent cation current in rat neocortical neurones. *J Physiol* **479**, 199–205.
- Berridge MJ, Lipp P & Bootman MD (2000). The versatility and universality of calcium signaling. *Nature Rev Mol Cell Biol* **1**, 11–21.
- Bobkov YV & Ache BW (2003). Calcium sensitivity of a sodium-activated nonselective cation channel in lobster olfactory receptor neurons. *J Neurophysiol* **90**, 2928–2940.
- Bradley J, Bonigk W, Yau KW & Frings S (2004). Calmodulin permanently associates with rat olfactory CNG channels under native conditions. *Nature Neurosci* **7**, 705–710.
- Cao YJ & Houamed KM (1999). Activation of recombinant human SK4 channels by metal cations. *FEBS Lett* **446**, 137–141.
- Chao S-H, Suzuki Y, Zysk JR & Cheung WY (1984). Activation of calmodulin by various metal cations as a function of ionic radius. *Mol Pharmacol* **26**, 75–82.
- Chen QX, Perkins KL, Choi DW & Wong RKS (1997). Secondary activation of a cation conductance is responsible for NMDA toxicity in acutely isolated hippocampal neurons. *J Neurosci* **17**, 4032–4036.
- Chen M & Simard JM (2001). Cell swelling and a nonselective cation channel regulated by internal Ca²⁺ and ATP in native reactive astrocytes from adult rat brain. *J Neurosci* **21**, 6512–6521.
- Cho H, Kim MS, Shim WS, Yang YD, Koo J & Oh U (2003). Calcium-activated cationic channel in rat sensory neurons. *Eur J Neurosci* **17**, 2630–2638.
- Colquhoun D, Neher E, Reuter H & Stevens CF (1981). Inward current channels activated by intracellular Ca in cultured cardiac cells. *Nature* **294**, 752–754.
- Colquhoun D & Sigworth FJ (1995). Fitting and statistical analysis of single channel records. In *Single Channel Recording*, 2nd edn, ed. Sakmann B & Neher E, pp. 483–587. Plenum, New York.
- Congar P, Leinekugel X, Ben-Ari Y & Crepel V (1997). A long-lasting calcium-activated nonselective cationic current is generated by synaptic stimulation or exogenous activation of group 1 metabotropic glutamate receptors in CA1 pyramidal neurons. *J Neurosci* **17**, 5366–5379.
- Conn PJ & Kaczmarek LK (1989). The bag cell neurons of *Aplysia*. *Mol Neurobiol* **3**, 237–273.
- Csanady L & Adam-Vizi V (2003). Ca²⁺- and voltage-dependent gating of Ca²⁺- and ATP-sensitive cationic channels in brain capillary endothelium. *Biophys J* **85**, 313–327.
- DeRiemer SA, Kaczmarek LK, Lai Y, McGuinness TL & Greengard P (1984). Calcium/calmodulin-dependent protein phosphorylation in the nervous system of *Aplysia*. *J Neurosci* **4**, 1618–1625.
- DeRiemer SA, Schweitzer B & Kaczmarek LK (1985). Inhibitors of calcium-dependent enzymes prevent the onset of afterdischarge in the peptidergic bag cell neurons of *Aplysia*. *Brain Res* **340**, 175–180.
- Egorov AV, Hamam BN, Fransen E, Hasselmo ME & Alonso AA (2002). Graded persistent activity in entorhinal cortex neurons. *Nature* **420**, 173–178.
- Fink LA, Connor JA & Kaczmarek LK (1988). Inositol triphosphate releases intracellularly stored calcium and modulates ion channels in molluscan neurons. *J Neurosci* **8**, 2544–2555.
- Fisher TE, Levy S & Kaczmarek LK (1994). Transient changes in intracellular calcium associated with a prolonged increase in excitability in neurons of *Aplysia californica*. *J Neurophysiol* **71**, 1254–1257.
- Fraser DD & MacVicar BA (1996). Cholinergic-dependent plateau potential in CA1 hippocampal pyramidal neurons. *J Neurosci* **16**, 4113–4128.

- Gietzen K, Sadorf I & Bader H (1982). A model for the regulation of the calmodulin-dependent enzymes erythrocyte Ca^{2+} -transport ATPase and brain phosphodiesterase by activators and inhibitors. *J Biochem* **207**, 541–548.
- Gonzalez-Perrett S, Batelli M, Kim K, Essafi M, Timpanaro G, Moltabetti N, Reisin IL, Arnaout MA & Cantiello HF (2002). Voltage dependence and pH regulation of human polycystin-2-mediated cation channel activity. *J Biol Chem* **277**, 24959–24966.
- Guinamard R, Chatelier A, Demion M, Potreau D, Patri S, Rahmati M & Bois P (2004). Functional characterization of a Ca^{2+} -activated non-selective cation channel in human atrial cardiomyocytes. *J Physiol* **558**, 75–83.
- Haiech J, Claude BBK & Demaille JJG (1981). Effects of cations on affinity of calmodulin for calcium: ordered binding of calcium ions allows for specific activation of calmodulin-stimulated enzymes. *Biochemistry* **20**, 3890–3897.
- Haj-Dahmane S & Andrade R (1997). Calcium-activated cation nonselective current contributes to the fast afterdepolarization in rat prefrontal cortex neurons. *J Neurophysiol* **78**, 1983–1989.
- Hall BJ & Delaney KR (2000). Contribution of a calcium-activated non-specific conductance to NMDA receptor-mediated synaptic potentials in granule cells of the frog olfactory bulb. *J Physiol* **543**, 819–834.
- Heierhorst J, Probst WC, Vilim FS, Buku A & Weiss KR (1994). Autophosphorylation of molluscan twitchin and interaction of its kinase domain with calcium/calmodulin. *J Biol Chem* **269**, 21086–21093.
- Hille B (2001). *Ionic Channels of Excitable Membranes*, 3rd edn. Sinauer, Sunderland, MA, USA.
- Kass RS, Lederer WJ, Tsien RW & Weingart R (1978). Role of calcium ions in transient inward currents and aftercontractions induced by strophanthidin in cardiac Purkinje fibres. *J Physiol* **281**, 187–208.
- Kononenko NI, Medin I & Dudek FE (2004). Persistent subthreshold voltage-dependent cation single channels in suprachiasmatic nucleus neurons. *Neuroscience* **129**, 85–92.
- Kramer RH & Zucker RS (1985). Calcium-dependent inward current in *Aplysia* bursting pace-maker neurones. *J Physiol* **362**, 107–130.
- Krupp JL, Vissel B, Thomas CG, Heinemann SF & Westbrook GL (1999). Interactions of calmodulin and α -actinin with the NR1 subunit modulate Ca^{2+} -dependent inactivation of NMDA receptors. *J Neurosci* **19**, 1165–1178.
- Kupfermann I (1967). Stimulation of egg laying: possible neuroendocrine function of bag cells of abdominal ganglion of *Aplysia californica*. *Nature* **216**, 814–815.
- Kupfermann I & Kandel ER (1970). Electrophysiological properties and functional interconnections of two symmetrical neurosecretory clusters (bag cells) in abdominal ganglion of *Aplysia*. *J Neurophysiol* **33**, 865–876.
- Lambers TT, Weidema AF, Nilius B, Hoenderop JGJ & Bindels RJM (2004). Regulation of the mouse epithelial Ca^{2+} channel TRPV6 by the Ca^{2+} -sensor calmodulin. *J Biol Chem* **279**, 28855–28861.
- Lan L, Bawden MJ, Auld AM & Barritt GJ (1996). Expression of *Drosophila* trpl cRNA in *Xenopus laevis* oocytes leads to the appearance of a Ca^{2+} channel activated by Ca^{2+} and calmodulin, and by guanosine 5' [γ -thio]triphosphate. *Biochem J* **316**, 793–803.
- Launay P, Fleig A, Perraud AL, Schareberg AM, Penner R & Kinet JP (2002). TRPM4 is a Ca^{2+} -activated nonselective cation channel mediating cell membrane depolarization. *Cell* **109**, 397–407.
- Levitan IB (1999). It is calmodulin after all! Mediator of the calcium modulation of multiple ion channels. *Neuron* **22**, 645–648.
- Levitan IB & Kaczmarek LK (2001). *The Neuron: Cell and Molecular Biology*, 3rd edn. Oxford University Press, New York.
- Liman ER (2003). Regulation by voltage and adenine nucleotides of a Ca^{2+} -activated cation channel from hamster vomeronasal sensory neurons. *J Physiol* **548**, 777–787.
- Liu M, Chen TY, Ahamed B, Li J & Yau KW (1994). Calcium-calmodulin modulation of the olfactory cyclic nucleotide-gated cation channel. *Science* **266**, 1348–1354.
- Liu D & Liman ER (2003). Intracellular Ca^{2+} and the phospholipids PIP_2 regulate the taste transduction ion channel TRPM5. *Proc Natl Acad Sci* **100**, 15160–15165.
- Llinas R, Sugimori M & Silver RB (1992). Microdomains of high calcium concentration in a presynaptic terminal. *Science* **256**, 677–679.
- Magoski NS (2004). Regulation of an *Aplysia* bag cell neuron cation channel by closely associated protein kinase A and a protein phosphatase. *J Neurosci* **24**, 6833–6841.
- Magoski NS & Kaczmarek LK (2005). Association/dissociation of a channel-kinase complex underlies state-dependent modulation. *J Neurosci* **25**, 8037–8047.
- Magoski NS, Knox RJ & Kaczmarek LK (2000). Activation of a Ca^{2+} -permeable cation channel produces a prolonged attenuation of intracellular Ca^{2+} release in *Aplysia* bag cell neurons. *J Physiol* **522**, 271–283.
- Magoski NS, Wilson GF & Kaczmarek LK (2002). Protein kinase modulation of a neuronal cation channel requires protein-protein interaction mediated by an Src homology 3 domain. *J Neurosci* **22**, 1–9.
- Michikawa T, Hirota J, Kawano S, Hiraoka M, Yamada M, Furuichi T & Mikoshiba K (1999). Calmodulin mediates calcium-dependent inactivation of the cerebellar type 1 inositol 1,4,5-trisphosphate receptor. *Neuron* **23**, 799–808.
- Miyashita T, Tatsumi H, Furuta H, Mori N & Sokabe M (2001). Calcium-sensitive nonselective cation channel identified in epithelial cells isolated from the endolymphatic sac of guinea pigs. *J Membr Biol* **182**, 113–122.
- Moreau B, Straube S, Fisher RJ, Putney JW Jr & Parekh AB (2005). Ca^{2+} -calmodulin-dependent facilitation and Ca^{2+} inactivation of Ca^{2+} release-activated Ca^{2+} channels. *J Biol Chem* **280**, 8776–8783.
- Morriset V & Nagy F (1999). Ionic basis for plateau potentials in deep dorsal horn neurons of the rat spinal cord. *J Neurosci* **19**, 7309–7316.
- Neher R (1998). Vesicle pools and Ca^{2+} microdomains: new tools for understanding their roles in neurotransmitter release. *Neuron* **20**, 389–399.

- Nilius B, Prenen J, Droogmans G, Voets T, Vennekens R, Freichel M, Wissenbach U & Flockerzi V (2003). Voltage dependence of the Ca²⁺-activated cation channel TRPM4. *J Biol Chem* **278**, 30813–30820.
- Nilius B, Prenen J, Tang J, Wang C, Owsianik G, Janssens A, Voets T & Zhu MX (2005). Regulation of the Ca²⁺ sensitivity of the nonselective cation channel TRPM4. *J Biol Chem* **280**, 6423–6433.
- Obukhov AG & Nowycky MC (2005). A cytosolic residue mediates Mg²⁺ block and regulates inward current amplitude of a transient receptor potential channel. *J Neurosci* **25**, 1234–1239.
- Ordaz B, Tang J, Xiao R, Salgado A, Sampieri A, Zhu MX & Vaca L (2005). Calmodulin and calcium interplay in the modulation of TRPC5 channel activity. *J Biol Chem* **280**, 30788–30796.
- Ozawa T, Sasaki K & Umezawa Y (1999). Metal ion selectivity for formation of the calmodulin-metal-target peptide ternary complex studied by surface plasmon resonance spectroscopy. *Biochim Biophys Acta* **1434**, 211–220.
- Partridge LD, Muller TH & Swandulla D (1994). Calcium-activated non-selective channels in the nervous system. *Brain Res Rev* **19**, 310–325.
- Partridge LD & Swandulla D (1987). Single Ca²⁺-activated cation channels in bursting neurons of *Helix*. *Pflugers Arch* **410**, 627–631.
- Partridge LD & Swandulla D (1988). Ca²⁺-activated non-specific cation channels. *Trends Neurosci* **11**, 69–72.
- Partridge LD, Thompson SH, Smith SJ & Connor JA (1979). Current–voltage relationships of repetitively firing neurons. *Brain Res* **164**, 69–79.
- Payne ME, Fong YL, Ono T, Colbran RJ, Kemp BE, Soderling TR & Means AR (1988). Calcium/calmodulin-dependent protein kinase II. Characterization of distinct calmodulin binding and inhibitory domains. *J Biol Chem* **263**, 7190–7195.
- Pinsker HM & Dudek FE (1977). Bag cell control of egg laying in freely behaving *Aplysia*. *Science* **197**, 490–493.
- Prawitt D, Monteilh-Zoller MK, Brixel L, Spangenberg C, Zabel B, Fleig A & Penner R (2003). TRPM5 is a transient Ca²⁺-activated cation channel responding to rapid changes in [Ca²⁺]_i. *Proc Natl Acad Sci U S A* **100**, 15166–15171.
- Razani-Boroujerdi S & Partridge LD (1993). Activation and modulation of calcium-activated non-selective cation channels from embryonic chick sensory neurons. *Brain Res* **623**, 195–200.
- Rekling JC & Feldman JL (1997). Calcium-dependent plateau potentials in rostral ambiguous neurons in the newborn mouse brain stem in vitro. *J Neurophysiol* **78**, 2483–2492.
- Rycroft BK & Gibb AJ (2004). Regulation of single NMDA receptor channel activity by alpha-actinin and calmodulin in rat hippocampal granule cells. *J Neurosci* **557**, 795–808.
- Saimi Y & Kung C (2002). Calmodulin as an ion channel subunit. *Annu Rev Physiol* **64**, 289–311.
- Smith SJ & Augustine GJ (1988). Calcium ions, active zones and synaptic transmitter release. *Trends Neurosci* **11**, 458–464.
- Smith MA, Herson PS, Lee K, Pinnock RD & Ashford MLJ (2003). Hydrogen-peroxide-induced toxicity of rat striatal neurones involves activation of a non-selective cation channel. *J Physiol* **547**, 417–425.
- Strubing C, Krapivinsky G, Krapivinsky L & Clapham DE (2001). TRPC1 and TRPC5 form a novel cation channel in mammalian brain. *Neuron* **29**, 645–655.
- Swandulla D & Lux HD (1985). Activation of a nonspecific cation conductance by intracellular Ca²⁺ elevation in bursting pacemaker neurons of *Helix pomatia*. *J Neurophysiol* **54**, 1430–1443.
- Tong Q, Zhang W, Conrad K, Mostoller K, Cheung JY, Peterson BZ & Miller BA (2006). Regulation of the transient receptor potential channel TRPM2 by the Ca²⁺ sensor calmodulin. *J Biol Chem* **281**, 9076–9085.
- Van Belle H (1981). A potent inhibitor of calmodulin-activated enzymes. *Cell Calcium* **2**, 483–494.
- Van den Abbeele T, Tran Ba Huy P & Teulon J (1994). A calcium-activated nonselective cationic channel in the basolateral membrane of outer hair cells of the guinea pig cochlea. *Pflugers Arch* **417**, 56–63.
- Wang C-LA (1985). A note on Ca²⁺ binding to calmodulin. *Biochem Biophys Res Comm* **130**, 426–430.
- Wilson GF, Magoski NS & Kaczmarek LK (1998). Modulation of a calcium-sensitive nonspecific cation channel by closely associated protein kinase and phosphatase activities. *Proc Natl Acad Sci U S A* **95**, 10938–10943.
- Wilson GF, Richardson FC, Fisher TE, Olivera BM & Kaczmarek LK (1996). Identification and characterization of a Ca²⁺-sensitive nonspecific cation channel underlying prolonged repetitive firing in *Aplysia* neurons. *J Neurosci* **16**, 3661–3671.
- Xia X-M, Fakler B, Rivard A, Wayman G, Johnson-Pais T, Keen JE, Ishii T, Hirschberg B, Bond CT, Lutsenko S, Maylie J & Adelman JP (1998). Mechanism of calcium gating in non-conductance calcium-activated potassium channels. *Nature* **395**, 503–507.
- Yellen G (1982). Single Ca²⁺-activated nonselective cation channels in neuroblastoma. *Nature* **296**, 357–359.
- Zhang S, Ehlers MD, Bernhardt JP, Su C-T & Haganir RL (1998). Calmodulin mediates calcium-dependent inactivation of N-methyl-D-aspartate receptors. *Neuron* **21**, 443–453.
- Zhang B, Wootton JF & Harris-Warrick RM (1995). Calcium-dependent plateau potentials in a crab stomatogastric ganglion motor neuron. II. Calcium-activated slow inward current. *J Neurophysiol* **74**, 1938–1946.
- Zitt C, Zobel A, Obukhov AG, Harteneck C, Kalkbrenner F, Luckhoff A & Schultz G (1997). Cloning and functional expression of a human Ca²⁺-permeable cation channel activated by calcium store depletion. *Neuron* **16**, 1189–1196.
- Zuhlke RD, Pitt GS, Deisseroth K, Tsien RW & Reuter H (1999). Calmodulin supports both inactivation and facilitation of L-type calcium channels. *Nature* **399**, 159–162.

Acknowledgements

The authors thank Ms S. L. Smith for excellent technical assistance, Drs A. S. Mak and L. Li for the gift of the pCAM vector as well as assistance with calmodulin purification, Dr J. A. Simpson for technical expertise on protein gel electrophoresis,

Ms N. M. Magoski for critical evaluation of previous drafts of the manuscript, and the two anonymous reviewers along with the reviewing editor, for providing constructive comments to improve the manuscript. The study was supported by an operating grant from the Canadian Institutes of Health Research to N.S.M.

Author's present address

D. A. Lupinsky: McGill University, Department of Neurology and Neurosurgery, Douglas Hospital Research Centre, Montreal, QC, Canada, H4H 1R3.